Hyperlipidemia and atherosclerosis associated with liver disease in ferrochelatase-deficient mice[1]

Vincent W. Bloks,* Torsten Plösch,* Harry van Goor,† Han Roelofsen,* Juul Baller,* Rick Havinga,* Henkjan J. Verkade,* Aad van Tol, Peter L. M. Jansen,§ and Folkert Kuipers[2,*]**

Departments of Pediatrics,* Pathology,† and Gastroenterology,§ Center for Liver, Digestive, and Metabolic Diseases, Groningen University Institute for Drug Exploration, University Hospital Groningen, 9700 RB Groningen, The Netherlands; and Department of Biochemistry,** Erasmus University, 3000 RD Rotterdam, The Netherlands

Abstract **Erythropoietic protoporphyria (EPP) is an inherited disorder of heme synthesis caused by deficiency of the mitochondrial enzyme ferrochelatase. EPP in humans is associated with liver disease, hypertriglyceridemia, and a low level of high density lipoprotein (HDL) cholesterol. To explore consequences of ferrochelatase deficiency in lipid metabolism, we have analyzed hepatic lipid content and plasma lipoprotein levels in chow-fed BALB/c mice homozygous (*fch/fch*) or heterozygous (*fch/+*) for a point mutation in the ferrochelatase gene and in wild-type controls (+/+). Livers of *fch/fch* mice show bile duct proliferation and biliary fibrosis, but bile formation is not impaired. The free cholesterol content of *fch/fch* livers is significantly increased when compared with *fch/+* and +/+ livers. Plasma cholesterol in *fch/fch* mice (9.9 ± 6.4 mM) is elevated when compared with *fch/+* and +/+ mice (2.9 ± 0.2 and 2.5 ± 0.3 mM, respectively), because of an increased cholesterol content in the very low density lipoprotein-sized fractions, whereas HDL cholesterol is reduced. The ratio of cholesteryl ester to free cholesterol is 4.3 ± 0.6, 3.3 ± 0.3, and 0.3 ± 0.1 in the plasma of +/+, *fch/+*, and *fch/fch* mice, respectively. The latter is not due to reduced lecithin:cholesterol acyltransferase activity in plasma of *fch/fch* mice but to the presence of lipoprotein-X (Lp-X), a particle composed of bile-type lipids usually seen only in cholestatic conditions. Expression of *mdr2*, essential for biliary phospholipid/cholesterol secretion, is increased in *fch/fch* livers. In spite of this, biliary phospholipid/cholesterol secretion is reduced relative to that of bile salts. It is postulated that an inability of bile salts to stimulate lipid secretion adequately leads to formation of Lp-X in this noncholestatic condition. Distinct atherosclerotic lesions were found in aged *fch/fch* mice. Thus, ferrochelatase deficiency in mice leads to liver disease associated with altered hepatic lipid metabolism, a characteristic hyperlipidemia, and development of atherosclerosis.**—Bloks, V. W., T. Plösch, H. van Goor, H. Roelofsen, J. Baller, R. Havinga, H. J. Verkade, A. van Tol, P. L. M. Jansen, and F. Kuipers. **Hyperlipidemia and atherosclerosis associated with liver disease in ferrochelatase-deficient mice.** ***J. Lipid Res.*** **2001.** 42: **41–50.**

Supplementary key words lipoprotein-X • very low density lipoprotein • high density lipoprotein • cholesterol • bile • *mdr2* P-glycoprotein • bile salt

Erythropoietic protoporphyria (EPP) is an inherited disorder of heme synthesis caused by deficiency of the mitochondrial enzyme ferrochelatase (EC 4.99.1.1), responsible for insertion of iron into protoporphyrin (PP) (1). Impaired ferrochelatase activity in humans with EPP results in increased PP concentrations in erythrocytes, blood, liver, and feces (1). Skin lesions after exposure to sunlight represent the hallmark of EPP. Liver disease is one of the complications that may occur in patients with EPP but hepatic manifestations of EPP are diverse (1, 2). About 40 different mutations in the human ferrochelatase gene have been described so far (3). It appears that only mutations that give rise to severe deficiencies of enzyme activity predispose to development of liver disease for which transplantation is indicated (4).

Elevated plasma triglyceride levels and low levels of high density lipoprotein (HDL) cholesterol have been reported in EPP patients (5), but underlying mechanism(s) are unknown. In the present study, we used a mouse model of EPP (6) to evaluate the effects of ferrochelatase deficiency on hepatic lipid metabolism and plasma lipoprotein levels. Mice homozygous (*fch/fch*) or heterozygous (*fch/+*) for a point mutation in the ferrochelatase gene were compared with wild-type (+/+) controls. Residual enzyme activity in various organs, including liver, is ~5% in *fch/fch* mice and ~60% in *fch/+* mice (6). We have found that *fch/fch* mice on a normal chow diet develop

Abbreviations: *acat-2*, acyl-CoA:cholesterol acyltransferase gene-2; *apoa-I*, apolipoprotein A-I gene; *apob*, apolipoprotein B gene; bsep, bile salt export pump; EPP, erythropoietic protoporphyria; *fch*, inactivating point mutation in ferrochelatase gene; *ldlr*, low density lipoprotein receptor gene; Lp-X, lipoprotein-X; *mdr2*, multidrug resistance gene-2.

[1] Part of this work has been presented at the 71st Scientific Sessions of the American Heart Association, November 1998, at Dallas, Texas, and has been published in abstract form (Kuipers et al. 1998. *Circulation.* **98:** I-591).

[2] To whom correspondence should be addressed at Groningen Institute for Drug Studies, CMC IV, Room Y2115, Academic Hospital Groningen, Hanzeplein 1, 9700 RB Groningen, The Netherlands.
e-mail: f.kuipers@med.rug.nl; Web page: www.LabPediatricsRug.nl

bile duct proliferation and biliary fibrosis with porto-portal bridging (7). Bile formation is not impaired in these animals: in fact, biliary bile salt secretion is markedly enhanced (7). Heterozygotes, on the other hand, show normal bile formation and a characteristic fat accumulation in hepatocytes (7), indicating that impaired ferrochelatase activity per se may indeed affect hepatic lipid metabolism. We have determined the effects of (partial) ferrochelatase deficiency on hepatic and plasma lipoprotein levels in mice. Data show that reduced ferrochelatase activity in heterozygous *fch/+* mice is associated with development of severe hepatic steatosis, while a marked hyperlipidemia, characterized by the presence of lipoprotein-X (Lp-X) and reduced HDL, is present in homozygous *fch/fch* mice. The latter is associated with the presence of atherosclerotic lesions.

MATERIALS AND METHODS

Mice

Male and female *fch/fch* and *fch/+* mice with a BALB/c background were generously supplied by X. Montagutelli (Institut Pasteur, Paris, France) for establishing a breeding program at the Central Animal Laboratory, Faculty of Medical Sciences (University of Groningen, Groningen, The Netherlands). The animals were kept in a temperature- and light-controlled environment and were protected from direct light by means of a yellow filter. Age-matched control BALB/c mice were purchased from Harlan BV (Zeist, The Netherlands). Control animals were kept under the same ad libitum dietary conditions (SRM-A; Hope Farms BV, Woerden, The Netherlands) for at least 3 weeks prior to experiments. Animals received humane care according to local guidelines: experimental procedures were approved by the local Ethics Committee for Animal Experiments.

Experimental procedures

Male mice, 12–14 weeks of age, were anesthetized with halothane. A large blood sample was collected by cardiac puncture and transferred to an ethylenediaminetetraacetic acid-containing tube. Plasma was obtained for lipid and lipoprotein analysis: an aliquot was frozen immediately for determination of lecithin: cholesterol acyltransferase (LCAT) activity. The liver was excised and weighed. Small portions were rapidly frozen in liquid nitrogen for isolation of RNA, a part was slowly frozen in isopentane for preparation of sections for examination by microscopy, and the remainder was stored for lipid analyses.

Separate groups of mice were used for determination of hepatic very low density lipoprotein (VLDL) triglyceride production rates, as previously described (8). In short, mice were fasted overnight, anesthetized with halothane, and, after collection of a basal blood sample (75 μl) by tail bleeding, Triton WR-1339 (12.5 mg per 100 μl) was intravenously administered via the penile vein. Subsequently, blood samples were collected at 1, 2, 3, and 4 h after Triton WR-1339 administration. The 4-h blood sample (~750 μl) was collected by cardiac puncture for VLDL isolation by density gradient ultracentrifugation.

Separate groups of *fch/fch*, *fch/+*, and *+/+* mice (n = 3 per group) were used for the collection of serum after a 16-h fast, for assessment of Lp-X as described below.

Aged *fch/fch* and *fch/+* mice (9–12 months) were used for evaluation of atherosclerotic plaques. For this purpose, the thorax was opened under Nembutal anesthesia and the heart was in situ perfused with phosphate-buffered saline at room temperature. The heart was then dissected out, cleaned of surrounding tissues, and stored in buffered formalin or rapidly frozen in isopentane until processed.

Lipid analyses

Plasma concentrations of total and free cholesterol, triglycerides, phospholipids, and free fatty acids were measured with commercially available kits, as previously described (8, 9). Pooled plasma samples of the three groups of mice were used for lipoprotein separation by fast protein liquid chromatography (FPLC) (9) or by density gradient ultracentrifugation according to Pietzsch et al. (10), using a Beckman (Fullerton, CA) Optima TLX tabletop ultracentrifuge.

Fresh serum samples were used for assessment of Lp-X, using a commercially available kit (Lp-X Rapidophor; Immuno AG, Vienna, Austria), according to the manufacturer's instructions. Agarose electrophoresis was performed after addition of Sudan black (0.2%, w/v) to plasma and the mixture was incubated for 15 min at 45°C. Thereafter, an equal volume of 0.5% agarose was added and the samples were applied to a 0.5% (w/v) agarose gel containing 100 mM Tris-HCl, pH 8.2. The gel was immersed in 50 mM barbital-HCl, pH 8.8, and electrophoresis was performed at 150 mA for 3 h.

Hepatic lipid content was measured as previously described (8, 9) after Bligh and Dyer (11) extraction. Hepatic phospholipid species were separated by thin-layer chromatography followed by quantification through measurement of anorganic phosphate as detailed by Böttcher, van Gent, and Pries (12).

Western blotting

Fractions separated by FPLC were taken for semiquantitative assessment of apolipoprotein B-100 (apoB-100), apoB-48, and apoA-I contents by Western blotting exactly as described by Voshol et al. (9).

RNA isolation and RT-PCR procedures

Tissue samples for isolation of RNA were snap frozen in liquid nitrogen and stored at −80°C. Samples were homogenized and total RNA was isolated using the Trizol method (GIBCO, Grand Island, NY) and the SV total RNA isolation system (Promega, Madison, WI), according to the manufacturer instructions. Integrity of RNA was confirmed by agarose gel electrophoresis, and RNA concentration was measured spectrophotometrically. Single-stranded cDNA was obtained from 12 μg of total RNA, using 80 U of Moloney murine leukemia virus reverse transcriptase, 16 μl of 5-fold concentrated buffer, 32 U of RNase inhibitor, 1.06 μg of random primer, and 8 μl of dNTP mix (10 mM) (all from Boehringer Mannheim, Indianapolis, IN) in a total volume of 80 μl, according to the manufacturer's instructions. Samples were incubated at 25°C for 10 min, at 45°C for 60 min, and at 95°C for 5 min. Reverse transcriptase-polymerase chain reaction (RT-PCR) for acyl-coenzyme A (CoA):cholesterol acyltransferase gene-2 (*acat-2*), low density lipoprotein (LDL) receptor gene (*ldlr*), apoA-I gene (*apoa-I*), and apoB gene (*apob*) was done in 25-μl volumes using 1.5 μl of cDNA, 0.125 μl (0.625 U) of *Taq* polymerase, 2.5 μl of 10-fold buffer, 0.5 μl of dNTP mix (10 mM) (all from Boehringer Mannheim), 1.0 μl of dimethyl sulfoxide (Merck, Rahway, NJ), and 0.5 μl of each primer (25 pmol; GIBCO). Primers used were GTG CCT GGG ATC TTT TGT GT and AAC ATC CTG TCT CCA AAC CG for *acat-2* (13), GGA GTG CAT CAG CTT GGA CA and GTG ATG CCA TTT GGC CAC TG for *ldlr* (14), GGC AGA GAC TAT GTG TCC CAG TTT GA and GTC ATC CAG CGC GGG TTT GGC CTT CTC for *apoa-I* (15), and GAC AGT GTC AAC AAG GCT TTG TAT TGG GT and TGA AGA CTC CAG ATG AGG AC for *apob* (15). PCR included a predenaturation at 95°C for 2 min

and a final extension of 5 min at 72°C. Amplification was done for 30 s at 95°C, annealing for 30 s at 56°C, and extension for 30 s at 72°C. This step was repeated 22 times for both *apoa-I* and *apob*. The PCR products were separated on an 2.5% agarose gel and the intensity of the ethidium bromide staining was measured with an Imagemaster VDS gel documentation system and Imagemaster 1D elite software (Pharmacia, Uppsala, Sweden).

Competitive PCR for 18S ribosomal RNA and *mdr2*

Homologous DNA competitors were generated according to the method by Celi, Zenilman, and Shuldiner (16). Briefly, a linker primer [CTG AAC GCC ACT TGT CCC TCA GAC AAA TCG CTG CAC CAA C for ribosomal RNA, TAT CCG CTA TGG CCG TGG GAA TCA TCA TGA AAC TGC CCC AGA for multidrug resistance gene-2(*mdr2*)], with half containing the final primer binding site and the other half being a nested primer for the gene, was used to generate a competitor that is identical to the natural PCR product, but slightly shorter. Its concentration was estimated on an agarose gel in comparison with the Boehringer Mannheim MWM XIV ladder. PCR for ribosomal RNA was done with a 1.5-μl sample of cDNA and 1.5 μl of a competitor dilution containing approximately 55×10^6 copies per microliter, under the same conditions as mentioned above, with primers CTA TTG CGC CGC TAG AGG TG and CTG AAC GCC ACT TGT CCC TC. The protocol used included 2 min of preheating at 95°C, 18 cycles of 95°C, 60°C, 72°C (30 s each), followed by a final extension of 5 min at 72°C. For *mdr2* [primers TAT CCG CTA TGG CCG TGG GAA and ATC GGT GAG CTA TCA CAA TGG (17)], 7,000 and 11,000 copies of the competitor per microliter were used, with an annealing temperature of 54°C and 30 cycles, but otherwise identical conditions. The products were measured as described above. The original abundance of the mRNA in the sample was calculated by taking the ratio of competitor to natural product, corrected for the lower size, and therefore for the lower ethidium bromide intercalation of the competitor.

Measurement of LCAT activity

Plasma LCAT activity levels were measured in duplicate, using excess exogenous substrate containing [^{3}H]cholesterol as described (18). The measured LCAT activity levels vary linearly with the amount of plasma added to the incubation mixture and are indicative of plasma LCAT concentrations. LCAT activity levels were related to the activities in a human plasma pool and expressed in arbitrary units, which correspond to the percentages of the activities present in the plasma pool. All animals were analyzed with one batch of substrates. LCAT activity was also measured with the endogenous substrate lipoproteins present in plasma, by assaying the rate of cholesterol esterification in whole plasma, as described previously (19).

Histological evaluation of liver and heart tissue

Frozen liver and heart sections were stained for neutral fat with oil red O and counterstained with hemotoxylin. Localization of *mdr2* P-glycoprotein (Pgp) and the bile salt export pump (bsep) was studied by confocal microscopy on 10-μm frozen liver sections, as described previously (20). Sections were fixed with 100% acetone for 10 min and air dried. Blocking was performed with 5% rabbit serum and the sections were then incubated with a 1:50 dilution of the P3II-26 antibody for *mdr2* Pgp and antibody K12 for bsep (20). Formalin-fixed heart sections were stained with Alcian blue by standard procedures.

Statistics

Comparison of data from +/+, *fch*/+, and *fch*/*fch* mice was done by analysis of variance and post hoc Newman-Keuls *t*-test. A *P* value of <0.05 was considered significant.

RESULTS

Hepatic lipid content

Livers of *fch*/*fch* mice show distinct bile duct proliferation and biliary fibrosis already at 2–3 months of age, whereas hepatocyte morphology appears normal at this age (7) (see also **Fig. 1**). Analysis of hepatic lipid content, summarized in **Table 1**, revealed a significant increase in free cholesterol content and in the sphingomyelin-to-phosphatidylcholine ratio in *fch*/*fch* mice in comparison with the other two groups. A marked accumulation of

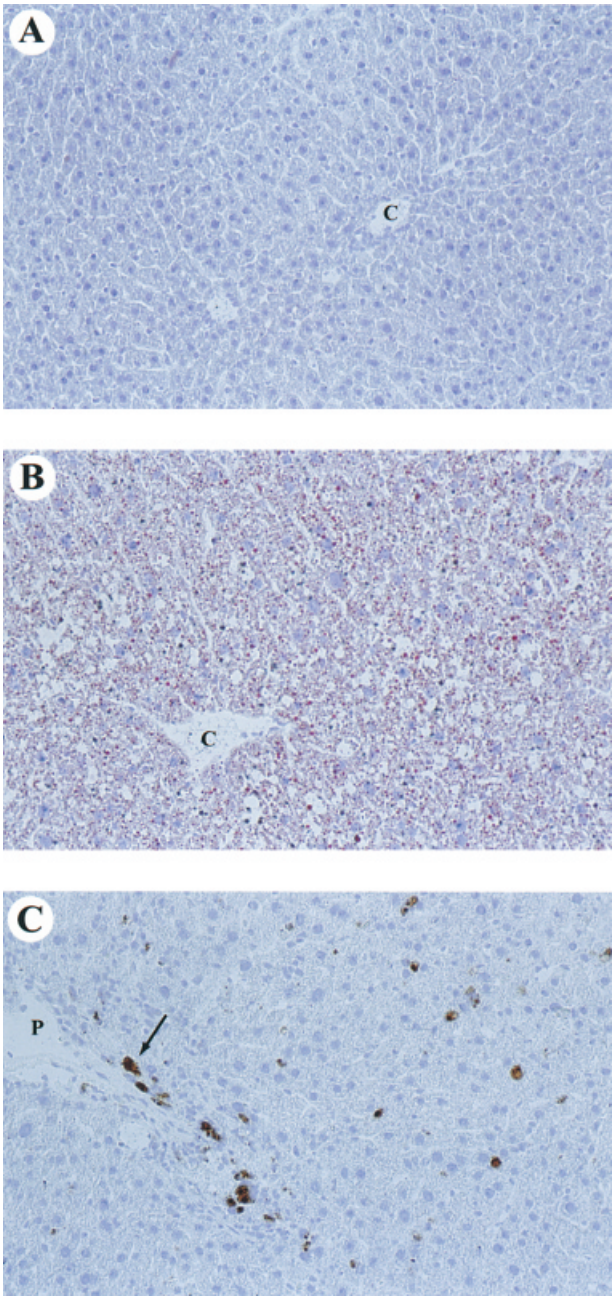

Fig. 1. Oil red O staining for neutral fat on frozen liver sections of male wild-type (A), *fch*/+ (B), and *fch*/*fch* (C) mice fed standard laboratory chow. Arrow in (C) indicates the presence of protoporphyrin deposits in *fch*/*fch* liver. C, Central vein; p, portal vein. Original magnification: ×40.

TABLE 1. Lipid content of livers of chow-fed wild-type male BALB/c mice (+/+) and of mice heterozygous (*fch/+*) or homozygous (*fch/fch*) for a point mutation in the ferrochelatase gene

	+/+	*fch/+*	*fch/fch*
Free cholesterol	24.1 ± 0.6	27.0 ± 1.3[a]	48.5 ± 6.0[b]
Cholesteryl ester	6.5 ± 1.0	26.6 ± 6.5[b]	15.4 ± 8.8[b]
Triglycerides	28.0 ± 11.3	216.2 ± 79.7[a,b]	27.2 ± 12.0
Phospholipids	255 ± 26	261 ± 29	277 ± 31
SM/PC ratio	0.91 ± 0.52	0.48 ± 0.24[a]	2.01 ± 0.08[b]

Values are in nmol/mg protein and represent means ± SD for five or six animals per group. SM, sphingomyelin; PC, phosphatidylcholine.
[a] Significant difference between *fch/+* and *fch/fch*.
[b] Significant difference from control values.

TABLE 3. Activity of LCAT, measured by two independent methods, in plasma of chow-fed wild-type male BALB/c mice (+/+) and of mice heterozygous (*fch/+*) or homozygous (*fch/fch*) for a point mutation in the ferrochelatase gene

	+/+	*fch/+*	*fch/fch*
LCAT[a] (% control)	54.5 ± 3.7	88.4 ± 4.2[b]	97.1 ± 12.6[b]
LCAT[c] (nmol/ml/h)	207.3 ± 16.9	317.3 ± 21.6[b]	312 ± 96

Values represent means ± SD of three to five animals per group. LCAT, lecithin:cholesterol acyltransferase.
[a] Expressed as percentage of activity measured in control plasma pool.
[b] Significant difference compared with control values.
[c] Expressed as rate of esterification of endogenous substrate.

hepatic triglycerides, that is, an 8-fold increase when compared with wild-type controls, is present in livers of *fch/+* mice but not in those of *fch/fch* mice. Staining of frozen liver sections for neutral lipid demonstrates that fat accumulates predominantly in perivenous hepatocytes, that is, cells surrounding the central vein, of *fch/+* livers (Fig. 1).

Plasma lipid concentrations and lipoprotein profiles

Plasma cholesterol levels are significantly higher in nonfasted *fch/fch* mice, ranging from 4.5 to 18.5 mM in male mice 2–3 months of age, than in *fch/+* and +/+ mice of similar age, with no difference between the latter two groups (**Table 2**). The ratio of cholesteryl ester to free cholesterol in plasma is profoundly decreased in *fch/fch* mice when compared with *fch/+* and +/+ mice, that is, 0.3 ± 0.1 ($P < 0.05$) versus 3.3 ± 0.3 and 4.3 ± 0.6, respectively. Plasma phospholipid concentrations are clearly increased in *fch/fch* mice when compared with the other two groups. Plasma triglyceride and fasting free fatty acid levels are similar across the three groups (Table 2).

Table 3 shows that LCAT activity, as measured by two independent methods, is increased rather than decreased in *fch/fch* animals in comparison with the other two groups, indicating that the low cholesteryl ester-to-free cholesterol ratio is not caused by a liver disease-related reduction in LCAT synthesis or secretion. Likewise, steady state mRNA levels of acyl-CoA:cholesterol acyltransferase 2, the cholesteryl ester-forming enzyme most abundantly present in liver (13), are not reduced in *fch/fch* mice (data not shown), in accordance with the elevated cholesteryl ester content in the livers of these animals (Table 1).

Separation of plasma lipoproteins by FPLC revealed that the characteristic HDL pattern of cholesterol in the +/+ mice is completely shifted toward the VLDL and intermediate density lipoprotein (IDL)/LDL-sized fractions in *fch/fch* mice (**Fig. 2A**). Free cholesterol is abundantly present in the VLDL-sized fractions in *fch/fch* mice (Fig. 2C), while the cholesteryl ester content of the HDL-sized fraction in these animals is clearly reduced in comparison with that in +/+ controls (Fig. 2B). Phospholipids are mainly present in the VLDL-sized fractions in *fch/fch* mice and in the HDL-sized fractions in +/+ mice (Fig. 2D). Finally, triglycerides that are almost exclusively associated with VLDL-sized fractions in +/+ mice are abundant in the IDL/LDL-sized fractions in *fch/fch* mice (Fig. 2E). Lipoprotein profiles in *fch/+* mice closely resemble those in +/+ mice (not shown).

Western blotting of fractions separated by FPLC revealed a markedly higher content of apoB-48 and B-100 in the VLDL- and IDL/LDL-sized lipoproteins in plasma of *fch/fch* mice than in that of +/+ mice (**Fig. 3**, bottom). ApoA-I contents in HDL-sized fractions appear somewhat reduced and show a shift toward smaller particle size in *fch/fch* mice (Fig. 3, top).

The presence of high free cholesterol and phospholipids in the VLDL-sized fractions in *fch/fch* mice on FPLC separation is compatible with the presence of Lp-X (21). To ascertain the presence of Lp-X in plasma of *fch/fch* mice, density gradient ultracentrifugation was performed. **Figure 4** shows that free cholesterol and phospholipids are mainly found in the LDL density range in *fch/fch* plasma, in contrast to the situation in +/+ plasma, in which lipid is mainly present in the HDL density range. Because Lp-X in mice consists of particles with VLDL size and LDL density (21), these data are interpreted to indicate that *fch/fch* plasma indeed contains Lp-X. The presence of Lp-X in fasting serum samples of *fch/fch* mice could be directly demonstrated by use of a precipitation assay (**Fig. 5A**), showing a clear precipitate that is not seen with control and *fch/+* serum. Agarose gel electrophoresis revealed the presence of a major band with low mobility in *fch/fch* plasma (Fig. 5B), reminiscent of the situation described in bile duct-ligated mice (21). No differences between control and *fch/+* plasma were seen.

TABLE 2. Lipid concentrations in plasma of chow-fed wild-type male BALB/c mice (+/+) and of mice heterozygous (*fch/+*) or homozygous (*fch/fch*) for a point mutation in the ferrochelatase gene

	+/+	*fch/+*	*fch/fch*
Total cholesterol	2.45 ± 0.29	2.95 ± 0.21[a]	9.85 ± 6.42[b]
Triglycerides	0.86 ± 0.28	1.50 ± 0.59	1.06 ± 0.34
Phospholipids	2.46 ± 0.36	3.35 ± 0.59	5.83 ± 1.04[b]
Free fatty acids[c]	1.03 ± 0.29	1.14 ± 0.15	1.17 ± 0.57

Values are in mmol/l and represent means ± SD for six animals per group.
[a] Significant difference between *fch/+* and *fch/fch*.
[b] Significant difference from control values.
[c] Plasma free fatty acid levels were measured after an overnight fast.

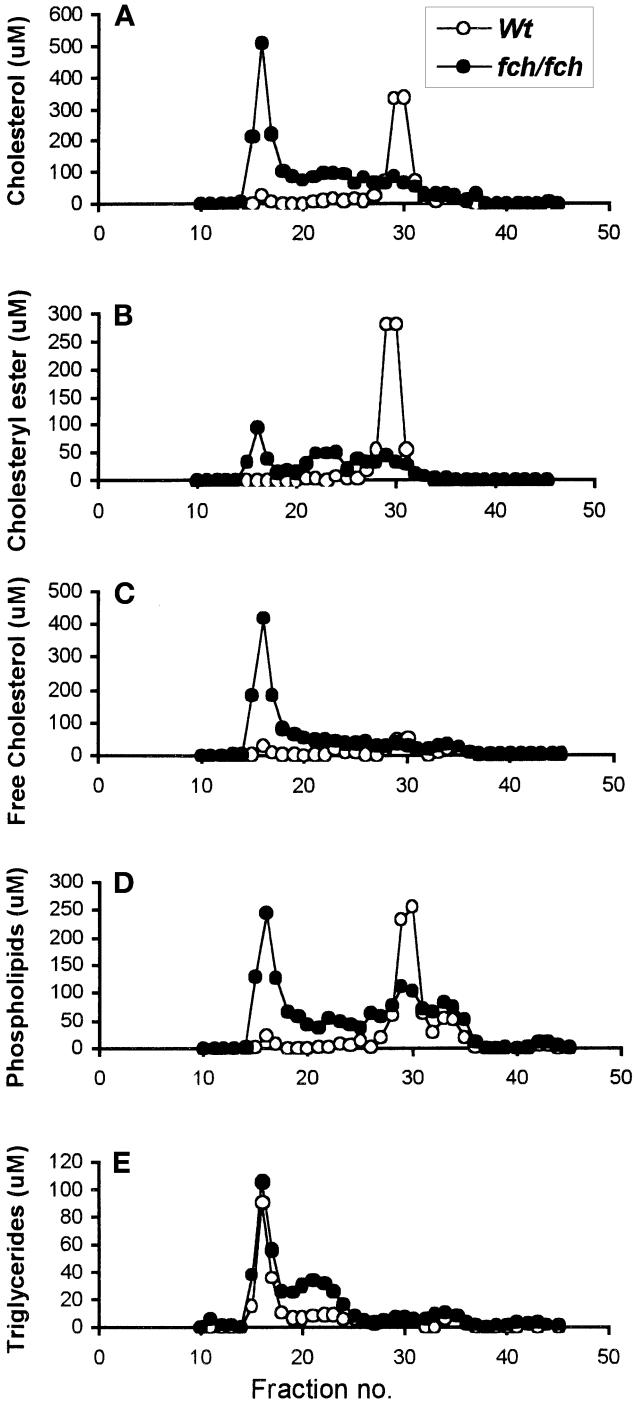

Fig. 2. Distribution of total cholesterol (A), cholesteryl ester (B), free cholesterol (C), phospholipids (D), and triglycerides (E) in male wild-type (open symbols) and *fch/fch* (closed symbols) mice. Pooled plasma samples were subjected to gel filtration using Superose 6 columns and lipid contents in each fraction were measured. Note that free cholesterol and phospholipids are predominantly present in the VLDL-sized fractions in *fch/fch* plasma. Profiles of *fch/+* mice were indistinguishable from those of wild-type mice and are not shown for reasons of clarity.

In vivo hepatic VLDL triglyceride production

To check whether increased VLDL production by the liver contributes to the high lipid and apoB levels in plasma of ferrochelatase-deficient mice, we measured VLDL triglyceride production by the Triton WR-1339 procedure. **Figure 6** shows the linear increase in plasma triglycerides in +/+, *fch/+*, and *fch/fch* mice on injection of Triton WR-1339: it is evident that this increase is less pronounced in *fch/fch* mice than in the other two groups. Calculation of hepatic VLDL triglyceride production rates from these concentrations, taking into account the fact that the plasma volume of *fch/fch* animals is somewhat larger than in the other groups (6), reveals a significantly lower value for *fch/fch* mice, that is, 0.086 ± 0.016 μmol/h/g body weight, than for +/+ and *fch/+* mice, that is, 0.121 ± 0.015 and 0.110 ± 0.029 μmol/h/g body weight, respectively. Analysis of lipid composition of VLDL particles isolated from plasma collected 4 h after Triton WR-1339 injection revealed that particles from *fch/fch* mice are relatively enriched in cholesteryl esters at the expense of triglycerides (**Table 4**).

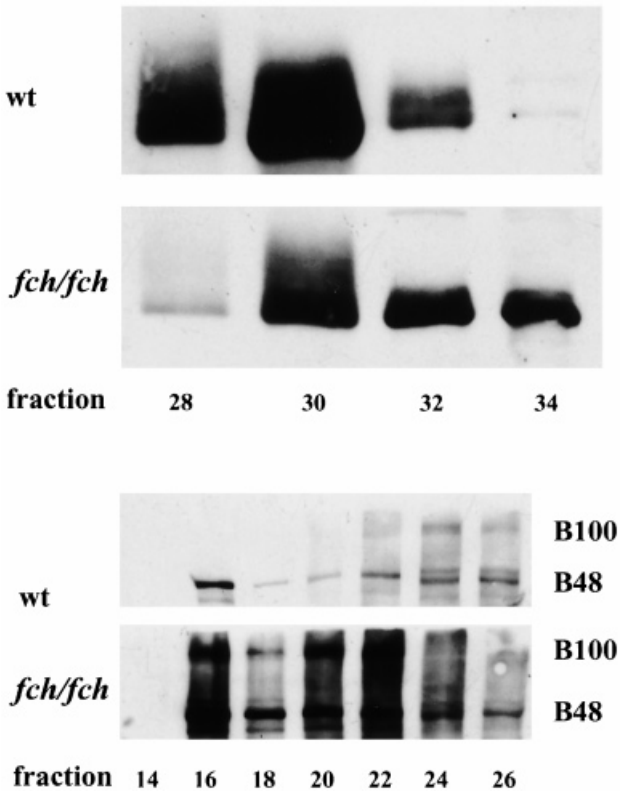

Fig. 3. Western blot analysis of apoA-I content of HDL-sized fractions 28–34 (top) and of apoB-100 and apoB-48 contents in VLDL/LDL-sized fractions 14–26 (bottom) after FPLC separation of wild-type and *fch/fch* mouse plasma (see Fig. 2). ApoB is clearly more abundant in VLDL/LDL-sized fractions of *fch/fch* plasma. The apoA-I content of HDL is somewhat reduced and shows a shift toward smaller particles in *fch/fch* plasma.

Hepatic mRNA levels of *apob* are similar in all three groups, as revealed by a semiquantitative RT-PCR procedure (**Fig. 7**).On the other hand, mRNA levels of *apoa-I* are increased in ferrochelatase-deficient mice (Fig. 7). In addition, steady state levels of *ldlr* mRNA, normalized to 18S mRNA, are increased by ~350% in *fch/fch* mice relative to controls (data not shown).

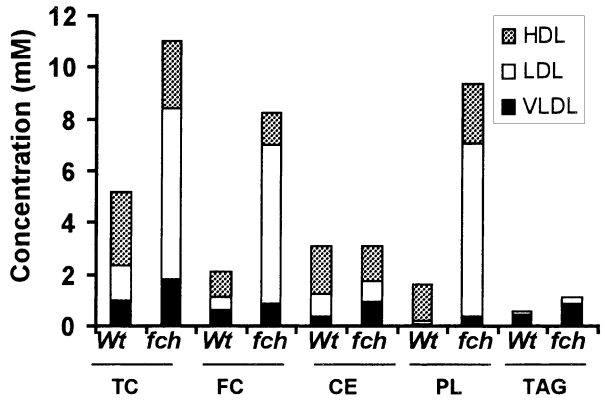

Fig. 4. Total cholesterol (TC), free cholesterol (FC), cholesteryl ester (CE), phospholipid (PL), and triglyceride (TAG) contents of high density lipoprotein (HDL; hatched bars), low density lipoprotein (LDL; open bars) and very low density lipoprotein (VLDL; solid bars) fractions isolated by density grandient ultracentrifugation from wild-type (*Wt*) and *fch/fch* (*fch*) mouse plasma. The majority of free cholesterol and phospholipids in *fch/fch* plasma is present in the LDL density fraction.

Bile formation and *mdr2* expression

The presence of Lp-X is a characteristic feature of cholestatic liver disease. Although plasma markers of liver disease (aspartate aminotransferase, alanine aminotransferase, bile salts) are elevated in *fch/fch* mice (7), these animals show increased bile flow and increased secretion of bile salts (7). In view of this, the presence of Lp-X is unexpected at first sight. Bile secretion of biliary lipids, that is, free cholesterol and phospholipids, is also increased in *fch/fch* mice when compared with +/+ and *fch/+* animals (**Fig. 8**). Yet, the increase in biliary lipid secretion is less pronounced than that of bile salt secretion, resulting in a significant increase in the bile salt-to-phospholipid plus cholesterol ratio in bile of these animals (Fig. 8), demonstrating a relative "undersecretion" of lipids into bile.

Because biliary lipid secretion critically depends on activity of *mdr2* Pgp and data have established that this transporter is also essential for Lp-X formation in bile duct-ligated mice (21), expression and localization of this protein were compared in +/+ and *fch/fch* mice. A competitive RT-PCR procedure revealed that *mdr*2 mRNA levels are slightly but significantly higher in *fch/fch* than in +/+ livers (Fig. 7). On immunohistochemistry, *mdr2* Pgp was found to be present in a canalicular staining pattern in *fch/fch* and +/+ liver (**Fig. 9**). Yet, staining in *fch/fch* liver appeared more diffuse than in +/+ liver: this "fuzzy" staining pattern has been interpreted to suggest localization in a pericanalicular vesicular compartment

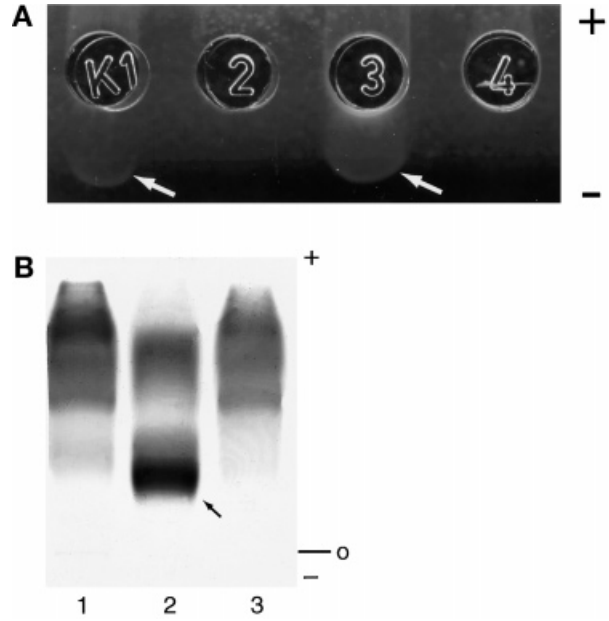

Fig. 5. A: Representative Lp-X precipitation assay showing precipitation in the gel on the cathode side in lane K1, containing positive control serum provided by the manufacturer, and in lane 3, containing serum of a fasted *fch/fch* mouse, as indicated by the white arrow. No precipitates are present in lanes 2 and 4, containing serum of fasted control and *fch/+* mice, respectively. +, Anode side of gel; –, cathode side of gel. B: Agarose gel electrophoresis of plasma samples from control (lane 1), *fch/fch* (lane 2), and *fch/+* (lane 3) mice. Plasma of *fch/fch* mice contains a characteristic band of low mobility, indicated by the arrow. O, Origin; +, anode side of gel; –, cathode side of gel.

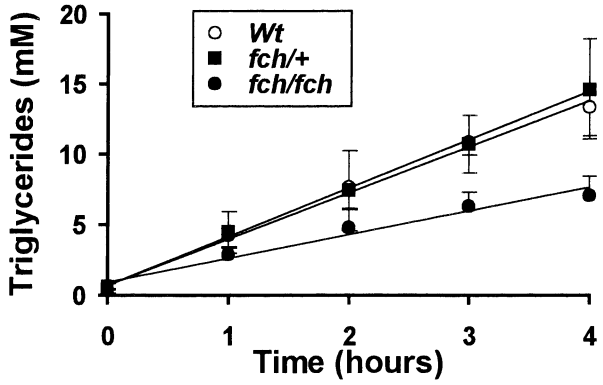

Fig. 6. Linear increase in plasma triglyceride concentration after intravenous administration of Triton WR-1339 in wild-type (*Wt*; open circles), *fch/+* (closed squares), and *fch/fch* (closed circles) mice. Mean values ± SD are shown for n = 4–7 per group.

TABLE 4. Lipid composition of VLDL particles isolated (d > 1.006) from plasma obtained 4 h after intravenous injection of Triton WR-1339 in chow-fed wild-type male BALB/c mice (+/+) or in mice heterozygous (*fch/+*) or homozygous (*fch/fch*) for a point mutation in the ferrochelatase gene

	+/+	*fch/+*	*fch/fch*
Free cholesterol	0.76 ± 0.13	0.83 ± 0.09	0.70 ± 0.03
Cholesteryl ester	0.18 ± 0.06	0.13 ± 0.07	0.71 ± 0.15[a]
Triglycerides	6.63 ± 1.71	6.92 ± 1.34	3.33 ± 0.43[a]
Phospholipids	1.47 ± 0.30	1.62 ± 0.22	1.68 ± 0.09

Values are in μmol/mg protein: protein content of the isolated very low density lipoprotein (VLDL) fractions was similar for the three groups, that is, 1.02 ± 0.21, 0.93 ± 0.16, and 0.90 ± 0.23 mg/ml for +/+, *fch/+*, and *fch/fch*, respectively. Values represent means ± SD of seven (+/+), four (*fch/+*) and four (*fch/fch*) isolations.

[a] Significant difference from control values.

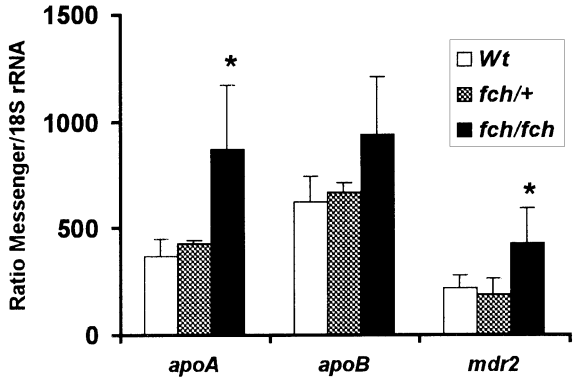

Fig. 7. Steady state mRNA levels of *apoa-I*, *apob*, and *mdr2* in livers of wild-type (*Wt*; open columns), *fch/+* (hatched columns), and *fch/fch* (solid columns) mice determined by reverse transcriptase-polymerase chain reaction. Values are normalized to 18S mRNA levels and represent mean values ± SD of three or four independent experiments. * Significantly different from control values.

(22, 23). A similar pattern was observed for the bsep (Fig. 9).

Atherosclerosis

In view of the atherogenic plasma lipid profile present in *fch/fch* mice, we screened sections of hearts obtained from relatively old (up to 12 months of age) mice for the presence of atherosclerotic lesions. Characteristic infiltrates with pigment-containing cells were present in hearts of *fch/fch* mice only (**Fig. 10A**); the nature of these cells has not been determined. Finally, characteristic lipid-containing lesions were present in the valve area of hearts of *fch/fch* mice on oil red O staining (Fig. 10B), indicative of the development of atherosclerosis. No lesions were found in hearts of *fch/+* mice.

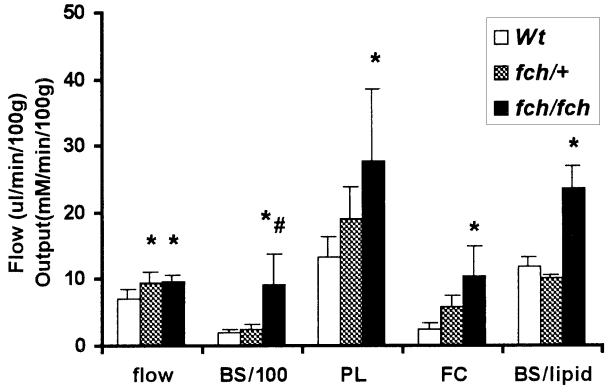

Fig. 8. Bile flow, biliary secretion rates of bile salts (BS/100), phospholipids (PL), and cholesterol (FC), and the ratio of biliary bile salts to phospholipids plus cholesterol (BS/lipid) in wild-type (open columns), *fch/+* (hatched columns), and *fch/fch* (solid columns) mice. Bile was collected after canulation of the gallbladder from anesthetized mice for a 30-min period. Mean values ± SD are shown for five or six animals per group. * Significantly different from control values; # significant difference between *fch/+* and *fch/fch* mice.

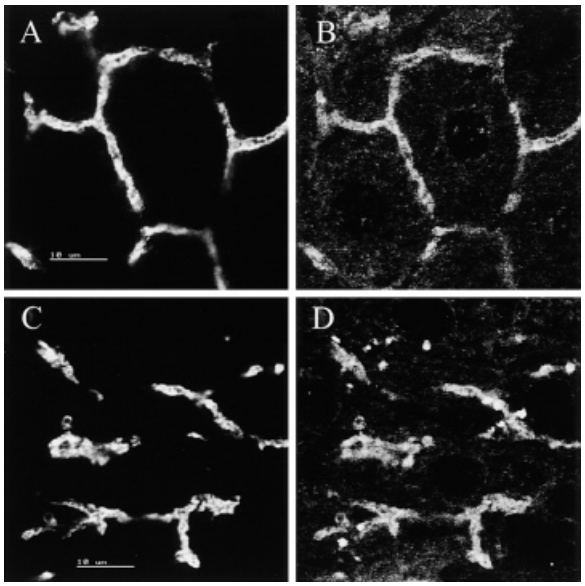

Fig. 9. Immunolocalization of the bile salt export pump (bsep; A and B) and *mdr2* Pgp (B and D) by confocal microscopy in livers from wild-type (A and C) and *fch/fch* (B and D) mice. Both bsep and *mdr2* Pgp show a distinct canalicular staining pattern in wild-type mice whereas staining in *fch/fch* mice has a "fuzzy" appearance. Bar indicates 10 μm.

DISCUSSION

This study shows that impaired activity of the mitochondrial enzyme ferrochelatase is associated with pronounced alterations in hepatic and plasma lipid concentrations in chow-fed mice. An ~50% reduction in enzyme activity leads to development of severe hepatic steatosis without significant effects on plasma lipid profiles and VLDL production in *fch/+* mice. Homozygous *fch/fch* mice show a marked hyperlipidemia, characterized by an increased content of cholesterol, triglycerides, apoB-100, and apoB-48 in VLDL/IDL-sized lipoproteins, reduced HDL cholesterol, and the presence of Lp-X. This combination is associated with the development of atherosclerotic lesions. Because some of these features have also been reported in patients with EPP, that is, low HDL and increased triglycerides in LDL/VLDL (5), it appears that impaired ferrochelatase activity per se and/or EPP-associated liver disease has unfavorable effects on plasma lipoprotein profiles. Whether or to what extent these effects are specific for EPP-associated liver disease cannot be determined with certainty on the basis of these experiments; in view of reduced hepatic iron content in *fch/fch* mice (7), however, it is highly unlikely that iron toxicity plays a role.

Hepatic steatosis, mainly confined to perivenous hepatocytes, is the only overt phenotypical feature of *fch/+* mice found so far. Steady-state plasma free fatty acid concentrations are not elevated in these animals, indicating that increased supply of fatty acids to the liver is not the cause of steatosis, as is the case in diabetes- or fasting-induced fatty liver. Preliminary findings have revealed that mitochondrial fatty acid β-oxidation may be impaired in

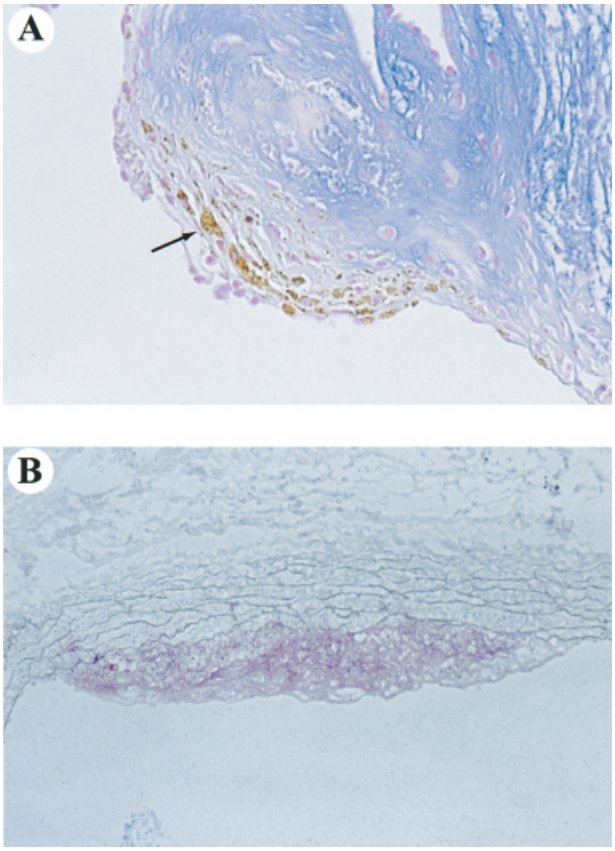

Fig. 10. A: Deposits of pigment-containing cells, indicated by the arrow, were present in hearts of aged *fch/fch* mice. Alcian blue staining, original magnification ×40. B: Oil red O staining for neutral fat on frozen sections demonstrates the presence of fat deposits in hearts of aged *fch/fch* mice. Original magnification: ×80.

these animals (T. Plösch, V. Bloks, and F. Kuipers, unpublished results). Homozygous *fch/fch* mice did not show hepatic triglyceride accumulation, which may reflect compromised fat metabolism associated with liver disease. On the other hand, livers of *fch/fch* mice do have increased free cholesterol content. This excess free cholesterol, which must be present in cellular membranes, is associated with a relative increase in hepatic sphingomyelin content: sphingomyelin is able to accommodate two times as much cholesterol as is phosphatidylcholine (24). An increase in sphingomyelin content of membrane fractions, in particular of microsomes, has also been reported in livers of rats rendered cirrhotic by exposure to phenobarbital-CCl_4 or by bile duct ligation (25), contributing to increased membrane rigidity in these models.

An intriguing finding of this study is the presence of Lp-X in plasma of the *fch/fch* mouse, as concluded on the basis of elevated plasma free cholesterol in the presence of high LCAT activity, elevated plasma phospholipids, the combination of FPLC and ultracentrifugation lipoprotein separation data, agarose gel electrophoresis, and a precipitation assay. Because these mice are not cholestatic in a functional sense and in fact show increased bile flow and biliary bile salt secretion, this study demonstrates, to the best of our knowledge for the first time, that Lp-X can be formed in the absence of obstructed bile flow in a situation in which LCAT is not deficient. The presence of Lp-X has so far been demonstrated only in animal models with experimentally induced cholestasis (21, 26) and in humans with cholestatic liver disease (27) as well as in subjects with LCAT deficiency (28). It is considered to represent a particle composed of bile-destined lipids redirected toward the plasma compartment in situations when bile flow is obstructed. Oude Elferink et al. (21) elegantly showed that formation of Lp-X in cholestatic mice critically depends on the presence of *mdr2* Pgp, the canalicular phospholipid translocator that is essential for biliary phospholipid secretion under normal conditions (29). Thus, *mdr2* Pgp-deficient mice do not form Lp-X on ligation of the common bile duct whereas mice overexpressing the human homolog (*MDR3*) show increased Lp-X formation under these experimental conditions (21). The authors speculate that *mdr2* Pgp present in subapical vesicles in cholestatic livers is active in phospholipid translocation into these vesicles followed by transcytosis toward the sinusoidal membrane and exocytosis to the blood compartment. Data of the present study support this option, because in *fch/fch* mice Lp-X is formed in the absence of biliary obstruction.

A major question that arises concerns the cause of Lp-X formation in *fch/fch* mice. In a previous study (7), we demonstrated that ferrochelatase-deficiency was associated with a strongly increased hepatobiliary bile salt flux. Bile salt secretion triggers the secretion of phospholipids and cholesterol into bile: the relationship between bile salt secretion on the one hand and phospholipid and cholesterol secretion on the other hand is curvilinear in nature in almost all species studied so far [see (30) and (31) for review]. The ability of bile salts to stimulate lipid secretion is critically dependent on the activity of *mdr2* Pgp (30, 31). It has been demonstrated that hepatic *mdr2* expression is induced when hepatic bile salt flux is increased by cholate feeding in rats (32). The current study shows that increased hepatic bile salt flux in *fch/fch* mice is also associated with increased *mdr2* expression. Yet, the amount of biliary cholesterol and phospholipids relative to that of bile salts is reduced in these animals, indicating that the coupling between the secretion rates of these bile constituents is disturbed. We speculate that the inability of bile salts to induce adequate phospholipid and cholesterol secretion into bile represents the mechanistic basis of Lp-X formation in *fch/fch* mice. Factors that may contribute to relative hyposecretion of biliary lipids include *a*) the presence of high concentrations of protoporphyrins in bile of these animals, which may interfere with the interactions between bile salts and the canalicular membrane; and *b*) altered composition of the canalicular membrane that interferes with the ability of bile salts to induce release of lipids from the membrane, for instance, because of a high sphingomyelin content (33). Alternatively, confocal microscopy revealed that *mdr2* Pgp in *fch/fch* liver may, in part, be present in a putative subapical compartment, reminiscent of the situation observed in bile duct-ligated mice (21). Thus, it may be that the relatively low lipid

secretion occurs because the *mdr2* Pgp content of the canalicular membrane is actually reduced. The presence of *mdr2* Pgp in the subapical compartment may be responsible for formation of Lp-X in this scenario.

In addition to the presence of Lp-X, hyperlipidemia in *fch/fch* mice is characterized by increased LDL cholesterol, triglycerides, and apoB, as well as reduced HDL cholesterol. Measurement of hepatic VLDL production by the Triton WR-1339 procedure revealed that the VLDL triglyceride production rate is reduced in these animals, predominantly because of the formation of small, triglyceride-poor particles. No change in hepatic *apob* mRNA levels was found, suggesting defective particle assembly as the underlying cause. The reason therefore remains unclear at the moment, and yet the data exclude increased VLDL production as a contributing factor in the development of hyperlipidemia. Part of the hyperlipidemia, therefore, is likely attributed to impaired lipolysis and/or clearance of lipoproteins in these animals in spite of increased hepatic LDL receptor expression. VLDL triglyceride production was not affected in *fch/+* mice, demonstrating that hepatic steatosis is not by definition associated with increased triglyceride secretion by the liver via this pathway. Low HDL cholesterol levels in *fch/fch* mice, in spite of increased hepatic *apoa-I* expression, remain unexplained at the moment. Low HDL is a common feature in human liver disease (34) but the underlying mechanism(s) have remained unclear.

Ferrochelatase deficiency in mice was found to be associated with the presence of pigment-containing cells in the heart, presumably reflecting deposition of protoporphyrin-laden macrophages. The pathological significance thereof, if any, is not known. In addition, distinct depositions of neutral fat-containing cells were found, indicating development of atherosclerosis in these mice. This may be due to high circulating levels of Lp-X, although the atherogenic potency of this aberrant particle has not been described. It is known, however, that Lp-X is not taken up by hepatocytes and is unable to downregulate cholesterol synthesis in HepG2 cells (35). Uptake seems to be limited to cells of the reticuloendothelial system (36), which may lead to deposition of lipid-laden macrophages. Low HDL cholesterol may contribute in this respect, as it will lead to reduced efflux and impaired reverse cholesterol transport from macrophages.

In conclusion, this study shows that ferrochelatase deficiency in mice leads to liver disease associated with a characteristic hyperlipidemia and atherosclerosis. Lp-X can be formed in conditions in which bile formation is not impaired and data indicate that disturbed biliary lipid secretion per se can give rise to Lp-X formation. The *fch/fch* mouse provides a model to evaluate the consequences of EPP-related liver disease and treatment thereof for lipid and lipoprotein metabolism.

This study was supported by grant WS 95-41 from The Netherlands Foundation for Digestive Diseases and by an Ubbo Emmius Scholarship (to T.P.). The authors thank Dr. X. Montagutelli and Prof. Dr. Y. Nordman (Institut Pasteur, Paris, France) for their generous gift of *fch* mice, and Ar Jansen (Central Animal Laboratory, University of Groningen) for taking care of the breeding program. Teus van Gent and Leo Scheek are thanked for performing the LCAT assays.

Manuscript received 7 April 2000 and in revised form 7 August 2000.

REFERENCES

1. Kappas, A., S. Sassa, and Y. Nordmann 1989. The porphyrias. *In* The Metabolic Basis of Inherited Disease. C. R. Scriver, A. L. Beadet, W. S. Sly, and D. Valle, editors. McGraw-Hill, New York. 1305–1365.
2. Cox, T. M. 1997. Erythropoietic protoporphyria. *J. Inherit. Metab.* **20:** 258–269.
3. Rufenacht, U. B., L. Gouya, X. Schneider-Yin, H. Puy, B. W. Schafer, R. Aquaron, Y. Nordmann, E. I. Minder, and J. C. Deybach. 1998. Systematic analysis of molecular defects in the ferrochelatase gene from patients with erythropoietic protoporphyria. *Am. J. Hum. Genet.* **62:** 1341–1352.
4. Bloomer, J., C. Bruzzone, L. Zhu, Y. Scarlett, S. Magness, and D. Brenner. 1998. Molecular defects in ferrochelatase in patients with protoporphyria requiring liver transplantation. *J. Clin. Invest.* **102:** 107–114.
5. Poh-Fitzpatrick, M. B., and R. H. Palmer. 1984. Elevated plasma triglyceride levels are associated with human protoporphyria. *J. Lab. Clin. Med.* **104:** 257–263.
6. Tutois, T., X. Montagutelli, V. Da Silva, H. Jouault, P. Rouyer-Fessard, K. Leroy-Viard, J. L. Guenet, Y. Nordmann, Y. Beuzard, and J. C. Deybach. 1991. Erythropoietic protoporphyria in the house mouse. *J. Clin. Invest.* **88:** 1730–1736.
7. Meerman, L., N. R. Koopen, V. Bloks, H. van Goor, R. Havinga, B. G. Wolthers, W. Kramer, S. Stengelin, M. Müller, F. Kuipers, and P. L. M. Jansen. 1999. Biliary fibrosis associated with altered bile composition in a mouse model of erythropoietic protoporphyria. *Gastroenterology.* **117:** 696–705.
8. Kuipers, F., M. C. Jong, Y. Lin, M. van Eck, R. Havinga, V. Bloks, H. J. Verkade, M. H. Hofker, H. Moshage, T. J. C. van Berkel, R. J. Vonk, and L. M. Havekes. 1997. Impaired secretion of very low density lipoprotein-triglyceride secretion in apolipoprotein E-deficient mice. *J. Clin. Invest.* **100:** 2915–2922.
9. Voshol, P. J., R. Havinga, H. Wolters, R. Ottenhof, H. M. G. Princen, R. P. J. Oude Elferink, A. K. Groen, and F. Kuipers. 1998. Reduced plasma cholesterol and increased fecal sterol loss in multidrug resistance gene 2 P-glycoprotein-deficient mice. *Gastroenterology.* **114:** 1024–1034.
10. Pietzch, J., S. Subat, S. Nitzche, W. Leonhardt, K. U. Schenkte, and M. Hanefeld. 1995. Very fast ultracentrifugation of serum lipoproteins: influence on lipoprotein separation and composition. *Biochim. Biophys. Acta.* **1254:** 77–88.
11. Bligh, E. G., and W. J. Dyer. 1959. A rapid method of total lipid extraction and purification. *Can. J. Biochem. Biophys.* **37:** 911–917.
12. Böttcher, C. F. J., C. M. van Gent, and C. Pries. 1961. A rapid and sensitive submicro-phosphorus determination. *Anal. Chim. Acta.* **24:** 203–204.
13. Cases, S., S. Novak, Y. W. Zheng, H. M. Myers, S. R. Lear, E. Sande, C. B. Welch, A. J. Lusis, T. A. Spencer, B. R. Krause, S. K. Erickson, and R. V. Farese, Jr. 1998. ACAT-2, a second mammalian acyl-CoA: cholesterol acyltransferase. Its cloning, expression and characterization. *J. Biol. Chem.* **273:** 26755–26764.
14. Polvino, W. J., D. A. Dichek, J. Mason, and W. F. Anderson. 1992. Molecular cloning and nucleotide sequence of cDNA encoding a functional murine low-density-lipoprotein receptor. *Somat. Cell Mol. Genet.* **18:** 443–450.
15. Shimano, H., J. D. Horton, R. E. Hammer, I. Shimomura, M. S. Brown, and J. L. Goldstein. 1996. Overproduction of cholesterol and fatty acids causes massive liver enlargement in transgenic mice expressing truncated SREBP-1a. *J. Clin. Invest.* **98:** 1575–1584.
16. Celi, F. S., M. E. Zenilman, and A. R. Shuldiner. 1993. A rapid and versatile method to synthetize internal standards for competitive PCR. *Nucleic Acids Res.* **21:** 1047.
17. Rappa, G., A. Lorico, M. C. Liu, C. D. Kruh, A. H. Cory, J. G. Cory, and A. C. Sartorelli. 1997. Overexpression of the multidrug resistance genes *mdr1*, *mdr3*, and *mrp* in L1210 leukemia cells resistant

to inhibitors of ribonucleotide reductase. *Biochem. Pharmacol.* **54:** 649–655.
18. Speijer, H., J. E. M. Groener, E. van Ramshorst, and A. van Tol. 1991. Different locations of cholesteryl ester transfer protein and phospholipid transfer proteins in plasma. *Atherosclerosis.* **90:** 159–168.
19. Dullaart, R. P. F., S. C. Riemens, L. Scheek, and A. van Tol. 1999. Insulin decreases plasma cholesteryl ester transfer but not cholesterol esterification in healthy subjects as wel as in normotriglyceridaemic patients with type 2 diabetes. *Eur. J. Clin. Invest.* **29:** 663–671.
20. Hooiveld, G. J. E. J., T. A. Vos, G. Scheffer, H. van Goor, H. Koning, V. Bloks, A. E. Loot, D. K. F. Meijer, P. L. M. Jansen, F. Kuipers, and M. Müller. 1999. 3-Hydroxy-3-methylglutaryl-coenzyme A reductase inhibitors (statins) induce expression of the phospholipid translocase mdr2 P-glycoprotein in rats. *Gastroenterology.* **117:** 678–687.
21. Oude Elferink, R. P. J., R. Ottenhof, J. van Marle, C. M. G. Frijters, A. J. Smith, and A. K. Groen. 1998. Class III P-glycoproteins mediate the formation of lipoprotein X in the mouse. *J. Clin. Invest.* **102:** 1749–1757.
22. Vos, T. A., G. J. E. J. Hooiveld, H. Koning, S. Childs, D. K. F. Meijer, H. Moshage, P. L. M. Jansen, and M. Müller. 1998. Up-regulation of the multidrug resistance genes, mrp1 and mdr1b, and down-regulation of the organic anion transporter, mrp2, and the bile salt transporter, spgp, in endotoxemic rat liver. *Hepatology.* **28:** 1637–1644.
23. Paulusma, C. C., M. J. Kothe, C. T. Bakker, P. J. Bosma, I. van Bokhoven, J. van Marle, U. Bolder, G. N. Tytgat, and R. P. J. Oude Elferink. 2000. Zonal down-regulation and redistribution of the multidrug resistance protein 2 during bile duct ligation in rat liver. *Hepatology.* **31:** 684–693.
24. Ohvo, H., C. Olsio, and J. P. Slotte. 1997. Effects of sphingomyelin and phosphatidylcholine degradation on cyclodextrin-mediated cholesterol efflux in cultured fibroblasts. *Biochim. Biophys. Acta.* **1349:** 131–141.
25. Reichen, J., J. T. Buters, Z. Sojcic, and F. J. Roos. 1992. Abnormal lipid composition of microsomes from cirrhotic rat liver—does it contribute to decreased microsomal function? *Experientia.* **48:** 482–486.
26. Felker, T. E., R. L. Hamilton, and R. J. Havel. 1978. Secretion of lipoprotein-X by perfused livers of rats with cholestasis. *Proc. Natl. Acad. Sci. USA.* **75:** 3459–3463.
27. Seidel, D., P. Alaupovic, and R. H. Furman. 1969. A lipoprotein characterizing obstructive jaundice. I. Method for quantitative separation and identification of lipoproteins in jaundiced subjects. *J. Clin. Invest.* **48:** 1211–1223.
28. Guerin, M., P. J. Dolphin, and M. J. Chapman. 1993. Familial lecithin:cholesterol acyltransferase deficiency: further resolution of lipoprotein particle heterogeneity in the low density interval. *Atherosclerosis.* **104:** 195–212.
29. Smit, J. J. M., A. H. Schinkel, R. P. J. Oude Elferink, A. K. Groen, E. Wagenaar, L. van Deemter, C. A. A. M. Mol, R. Ottenhof, N. M. T. van der Lugt, M. A. van Roon, M. A. van der Valk, G. J. A. Offerhaus, A. J. M. Berns, and P. Borst. 1993. Homozygous disruption of the murine mdr2 P-glycoprotein gene leads to a complete absence of phospholipid from bile and liver disease. *Cell.* **75:** 451–462.
30. Kuipers, F., R. P. J. Oude Elferink, H. J. Verkade, and A. K. Groen. 1997. Mechanisms and (patho)physiological significance of biliary cholesterol secretion. *Subcell. Biochem.* 295–318.
31. Oude Elferink, R. P. J., G. N. J. Tytgat, and A. K. Groen. 1997. The role of mdr2 P-glycoprotein in hepatobiliary lipid transport. *FASEB J.* **11:** 19–28.
32. Frijters, C. M. G., R. Ottenhof, M. J. A. van Wijland, C. M. J. van Nieuwkerk, A. K. Groen, and R. P. J. Oude Elferink. 1997. Regulation of mdr2 P-glycoprotein expression by bile salts. *Biochem. J.* **321:** 389–395.
33. Van Erpecum, K. J., and M. C. Carey. 1997. Influence of bile salts on molecular interactions between sphingomyelin and cholesterol: relevance to bile formation and stability. *Biochim. Biophys. Acta.* **1345:** 269–282.
34. Jahn, C. E., E. J. Schaefer, L. A. Taam, J. H. Hoofnagle, F. T. Lindgren, J. J. Albers, E. A. Jones, and H. B. Brewer, Jr. 1985. Lipoprotein abnormalities in primary biliary cirrhosis. Association with hepatic lipase inhibition as well as altered cholesterol esterification. *Gastroenterology.* **89:** 1266–1278.
35. Edwards, C. M., M. P. Otal, and P. W. Stacpoole. 1993. Lipoprotein X fails to inhibit hydroxymethylglutaryl coenzyme a reductase in HepG2 cells. *Metabolism.* **42:** 807–813.
36. Walli, A. K., and D. Seidel. 1984. Role of lipoprotein X in the pathogenesis of cholestatic hypercholesterolemia. *J. Clin. Invest.* **74:** 867–879.